Annals of Glaciology 35 2002

Annual-layer determinations and 167 year records of past climate of H72 ice core in east Dronning Maud Land, Antarctica

Fumihiko NISHIO,[1] Teruo FURUKAWA,[2] Gen HASHIDA,[2] Makoto IGARASHI,[2] Takao KAMEDA,[3] Mika KOHNO,[2] Hideaki MOTOYAMA,[2] Kazuhiro NAOKI,[4] Kazuhide SATOW,[5] Keisuke SUZUKI,[6] Morimasa TAKATA,[2] Yoko TOYAMA,[1] Tomomi YAMADA,[7] Okitsugu WATANABE[2]

[1]*Center for Environmental Remote Sensing, Chiba University, Yayoi-cho, Inage-ku, Chiba 263-8522, Japan*
E-mail: fnishio@ceres.cr.chiba-u.ac.jp
[2]*National Institute of Polar Research, Kaga, Itabashi-ku, Tokyo 173-8515, Japan*
[3]*Kitami Institute of Technology, Koen-cho 165, Kitami, 090-8507, Japan*
[4]*Hokkaido University of Education, Shiroyama 1-15-55, Kushiro 085-0826, Japan*
[5]*Nagaoka Technical College, 888, Nisikatagaicho, Nagaoka 940-8532, Japan*
[6]*Department of Environmental Sciences, Faculty of Science, Shinshu University, 3-1-1, Asahi, Matsumoto, Nagano 390-8621, Japan*
[7]*Institute of Low Temperature Science, Kita 18, Nishi 8, Sapporo, Hokkaido 060-0819, Japan*

ABSTRACT. To determine annual layers for reconstructing the past environment at annual resolution from ice cores, we employed snow-stake data back to 1972, tritium content, solid electrical conductivity measurements (ECM) and stratigraphic properties for the 73 m ice core at the H72 site, east Dronning Maud Land, Antarctica. The average annual surface mass balance at H72 is 307 mm a^{-1} w.e. during the last 27 years from continuous accumulation data, 317 mm a^{-1} w.e. according to the densification model and 311 mm a^{-1} w.e. according to the average surface mass balance for 167 years based on annual-layer counting. The ECM age is closely coincident with tritium age, and corresponds with the snow-stake record back to AD 1972 from the surface to 15 m depth. The H72 ice core is dated as AD 1831 by ECM at 73.16 m depth. The time series of yearly surface mass balance at H72 shows an almost constant 311 mm a^{-1} w.e. for the last 167 years. The oxygen-isotope records indicate a significant trend to lower values, with negative gradient of 1.7‰ (100 years)$^{-1}$.

1. INTRODUCTION

Japanese Antarctic Research Expeditions (JARE) have collected data on surface elevation, ice thickness, ice velocity, snow accumulation rate, snow temperature–depth profiles, stratigraphic and density profiles, surface snow features and paleo-environmental record from shallow ice cores along the traverse routes from Syowa station to Dome Fuji in east Dronning Maud Land. It is now possible to discuss the variation of proxy climate records of temperature and also precipitation in the Shirase drainage basin, which originates at Dome Fuji. This record is useful for predicting mass-balance change as a result of future global climatic change.

To evaluate the changes in past climate and surface mass balance of the ice sheet, shallow (100–200 m depth) ice coring has been conducted at several locations in the last decade. These cores are part of the International Trans-Antarctic Scientific Expedition (ITASE) program, which plans to extend the Antarctic record of change in climate, atmospheric chemistry and surface mass balance back to about 200 years ago, and contribute to an understanding of the interaction between global change and the Antarctic continent.

Studies on shallow ice cores are focused on dating layers and determining the specific layer for absolute dating using unique stratigraphic markers. Development of an annually resolved ice-core series is recognized as an essential component of the ITASE program because of the need for comparison. Several methods have been used to date the ice cores, in order to strengthen the interpretation. These include annual-layer counting of stable isotopes, chemistry, solid electrical conductivity measurements (ECM) and stratigraphic properties. These annual-layer counting methods are calibrated using volcanic and nuclear fallout markers. Stable-isotope measurements of ice ($\delta^{18}O$) have classically been employed as a proxy for temperature and accumulation by annual-layer counting in the dry snow zones of Antarctica and Greenland. Measurements of recent annual accumulation using snow stakes have been undertaken to provide a comparison with direct measurements of snow surface temperature time series and accumulation rate derived from ice-core analysis.

It is essential to determine annual layers to reconstruct the past environment from ice cores. We employed snow-stake data back to AD 1972, tritium content, solid ECM and stratigraphic properties for the H72 ice core. In this paper, we report how we determined the annual layers of the H72 ice core, and present results of surface mass balance and chemical components for the past 167 years from this site.

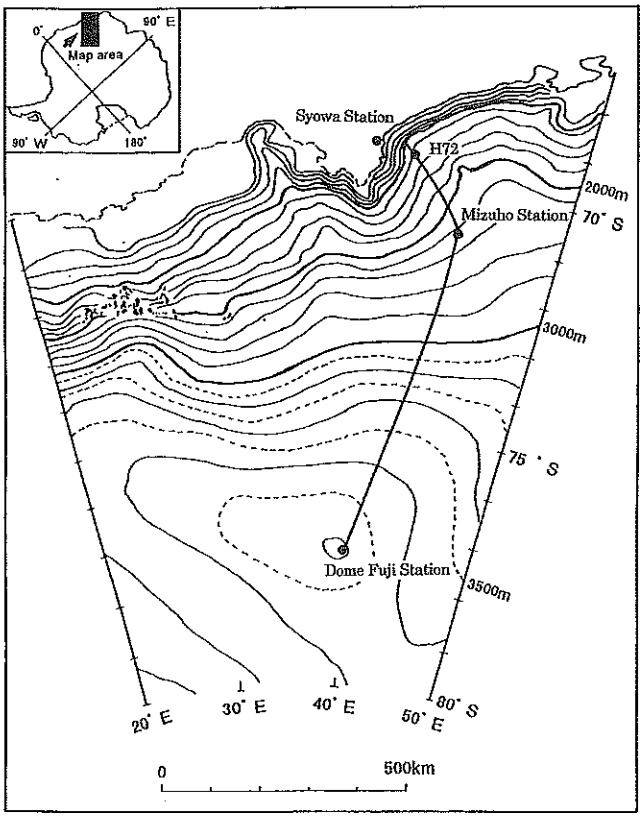

Fig. 1. Map of location of H72 core site, east Dronning Maud Land, Antarctica.

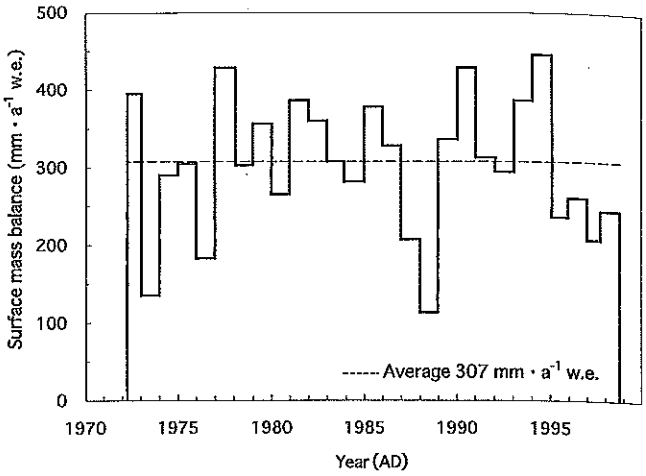

Fig. 2. Surface mass balance at H72 by snow-stake method (April 1972–October 1998).

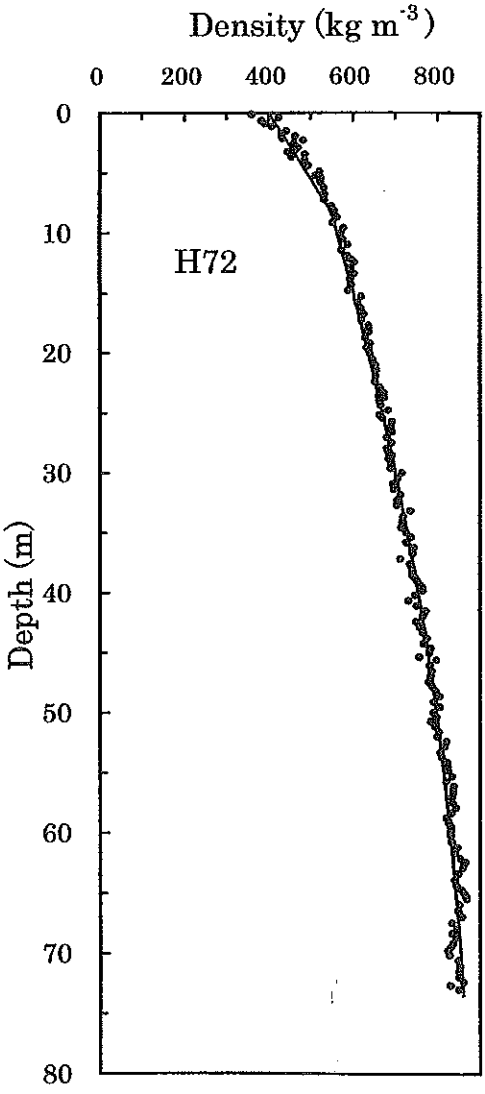

Fig. 3. Depth–density data with calculated profile by Herron and Langway (1980).

2. CORING SITE AND SURFACE MASS BALANCE DURING RECENT DECADES

The 73 m ice core was obtained in September 1998 at H72, (69°12′17″ S, 41°05′26″ E; 1214 m a.s.l.) in east Dronning Maud Land, Antarctic ice sheet (Fig. 1), by JARE-39 (Japanese Antarctic Research Expedition, 1999). Figure 2 shows the surface mass balance at H72 from AD 1973 to 1998 by the stake method. Data from each year have been published in JARE data reports (Yamada and others, 1975; Yokoyama, 1975; Satow, 1977; Fujii, 1978; Nishio, 1978; Wada and others, 1981; Kobayashi and others, 1982; Satow and others, 1983; Nakawo and others, 1984; Takahashi, 1984; Fujii and others, 1986, 1995; Ageta and others, 1987; Nishio and others, 1988; Nishio and Omae, 1989; Watanabe and others, 1990; Kamiyama and others, 1994; Motoyama and others, 1995, 1999; Shiraiwa and others, 1996; Azuma and others, 1997).

It is often observed in the coastal region of east Dronning Maud Land that snow does not accumulate every year, due to strong katabatic winds (Watanabe, 1978). However, annual surface mass balance at H72 is always positive and the average surface mass balance during the 26 year period April 1972–October 1998 is 307 mm a^{-1} w.e. Because H72 is located at the point where the mean surface slope changes from 0.8° (H72 to 2 km upstream area) to 0.3° (H72 to 2 km downstream area), it seems that snow tends to accumulate at the base of this gentle slope. We found only five sites at which >200 mm a^{-1} of snow accumulates every year along the traverse route between S16 (550 m a.s.l.) and Mizuho station (2260 m a.s.l.) using 17 years (AD 1973–89) of snow-stake data. These amount to only 4% of the snow-stake sites along the route (Osada, 1994). Thus, annually resolved climatic and environmental data in east Dronning Maud Land can be obtained from analyses of the H72 ice core.

Table 1. Volcanic signals and their chemical compositions found in the H72 ice core, and their probable source volcanoes

Signal labeled	Depth Top m	Depth Bottom m	Chemical composition $nssSO_4^{2-}$ µmol L^{-1}	pH	H^+ µmol L^{-1}	MSA µmol L^{-1}	Reliability as a volcanic signal	Characteristics of signals $nssSO_4^{2-}$	Characteristics of signals ECM	ECM age	Probable source volcano (eruption year)	VEI	Difference between volcanic event and ECM age
a	4.115	4.365	0.44	5.43	3.72	0.052	3		B	1992	Pinatubo (1991)?, Cerror Hudson (1991)?	6,5	+1
b	6.725	6.960	1.47	5.45	3.55	0.015	3	B		1988			
c	9.115	9.335	0.34	5.48	3.31	0.017	3		B	1983	El Chichón (1982)?, Galunggung (1982) ?	5,4	+1
d	15.000	15.240	0.66	5.33	4.68	0.025	3		B	1972	Deception Island? (1970)	3	+1
e	19.150	19.395	0.75	5.01	9.77	0.050	2		A	1964	Agung (1963)	4	+1
f	24.330	24.495	0.97	5.31	4.90	0.042	2	A	B	1955	Carran-Los Venados (1955)	4	0
g	38.500	38.640	0.71	5.11	7.76	0.072	2		A	1921	Kelut (1919), Manam (1919)	4	+2
h	47.150	47.285	0.86	5.32	4.79	0.077	3	B		1902	Santa Maria (1902)?	6	0
i	53.675	53.835	0.80	5.24	5.75	0.028	1	A	A	1886	Tarawera (1886)	5	0
j	54.320	54.485	0.88	5.29	5.13	0.026	1	A	A	1884	Krakatu (1883)	6	+1
k	57.755	57.875	0.78	5.33	4.68	n.d.[1]	3	B		1875	Merapi (1872)?	4	+3
l	58.610	58.730	0.78	5.25	5.62	0.009	1	A	A	1872			
m	63.780	63.905	1.01	5.27	5.37	0.031	1	A	A	1859	Fuego (1856)	4	+3
n	64.275	64.400	1.51	5.21	6.17	0.010	1	A	A	1858	Fuego (1856)	4	+2
o	66.675	66.800	0.81	5.35	4.47	0.043	3	B		1850			
p	70.990	71.090	1.09	5.24	5.75	0.032	1	A	A	1837	Cosiguina (1835)	5	+2

[1]n.d. = not detected; the minimum detection level is 0.006 µmol L^{-1}.

3. AGE DETERMINATION OF THE H72 ICE CORE

3.1. Densification model

The 10 m snow temperature at H72 is estimated to be −20.3°C based on the 10 m depth snow-temperature distribution in east Dronning Maud Land (Satow, 1978). Bulk density of the entire ice core was measured using an electronic balance, a scale and a caliper. It was measured from the surface to the core bottom (73.285 m depth) at about 40 cm intervals. Figure 3 shows the ice-core density data with a "best-fit" profile by the empirical densification model of Herron and Langway (1980). An average surface mass balance of 317 mm a^{-1} w.e. is obtained from the model. For the above calculations, the following values are used: surface snow density (400 kg m^{-3}), 10 m snow temperature (−20.3°C), ice density ρ_i (917 kg m^{-3}), k_1 (0.0218 m^{-1}) and the slope of the second stage of the densification profile (0.0355 m^{-1}). The parameter k_1 is defined by equation (6b) in Herron and Langway (1980), and "second stage" refers to the density region 550–800 kg m^{-3}.

3.2. Time markers by volcanic events

The acid concentration derived from H_2SO_4, HCl and HF is higher in the ice-core signals from volcanic eruptions (e.g. Hammer, 1980; Legrand and Delmas, 1987; Moore and others, 1991). We found several high peaks of SO_4^{2-} and Cl^- in the H72 ice core, but these signals do not indicate significant peaks of elevated concentration. We consider that the peaks of Cl^- are not of volcanic origin but probably originate from sea water since the ratios of Cl^- to Na^+ at all peaks are similar to that of sea water. The SO_4^{2-} has several origins (e.g. sea water, marine biogenic dimethylsulfide (DMS) and volcanic eruptions). We employed the profile of non-sea-salt SO_4^{2-} (hereafter $nssSO_4^{2-}$) concentration to detect volcanic signals. The $nssSO_4^{2-}$ in the H72 ice core indicates a periodic seasonal fluctuation caused by marine biogenic DMS, and the maximum value occurs during summer (Ayers and others, 1991; Osada, 1994; Koga and Tanaka, 1996). The highest values are almost the same level as the 2σ level (0.76 µmol L^{-1}) of $nssSO_4^{2-}$ data from the surface to the bottom (73.16 m depth).

We found 11 spike-like signals exceeding 2σ in the $nssSO_4^{2-}$ data and assume that these peaks are candidates for volcanic signals. Using pH and methanesulfonic acid (MSA) concentration at the same depth, we classified the spikes into two categories since methanesulfonic acid (MSA) is formed by atmospheric oxidation of DMS (Savoie and others, 1992). The characteristics of the two categories are as follows. In category A, the $nssSO_4^{2-}$ value exceeds 2σ, and both pH and MSA are lower than their average values (5.32 and 0.046 µmol L^{-1}, respectively); therefore, these signals show the highest reliability in volcanic signals. In category B, the $nssSO_4^{2-}$ value exceeds 2σ, and either the pH or MSA is higher than its average value. These signals show lower reliability than category A as indicators of volcanic signals.

We also employed ECM current to detect volcanic signals since ECM current reflects acidity in ice cores (e.g. Hammer, 1980). ECM current depends on ice-core density, showing a lower background current at a shallow depth of 24 m (density ~650 kg m^{-3}) than in deeper sections. The spike-like signals in ECM current exceeding 2σ (1.41 µA above 24 m depth, and 2.76 µA below 24 m) are considered to be derived from volcanic acids such as H_2SO_4, HCl, HF (Clausen and others, 1997). Using H^+ concentration at the same depth, we classified these spikes into two categories as follows. In category A, ECM current is $>2\sigma$ and H^+ concentration is high; therefore, these signals show the highest reliability as indicators for volcanic signals. The signals in category B have ECM current $>2\sigma$, but the H^+ concentration is lower than average (5.01 µmol L^{-1}); they have a lower reliability as volcanic indicators.

Using the two procedures described above, reliability

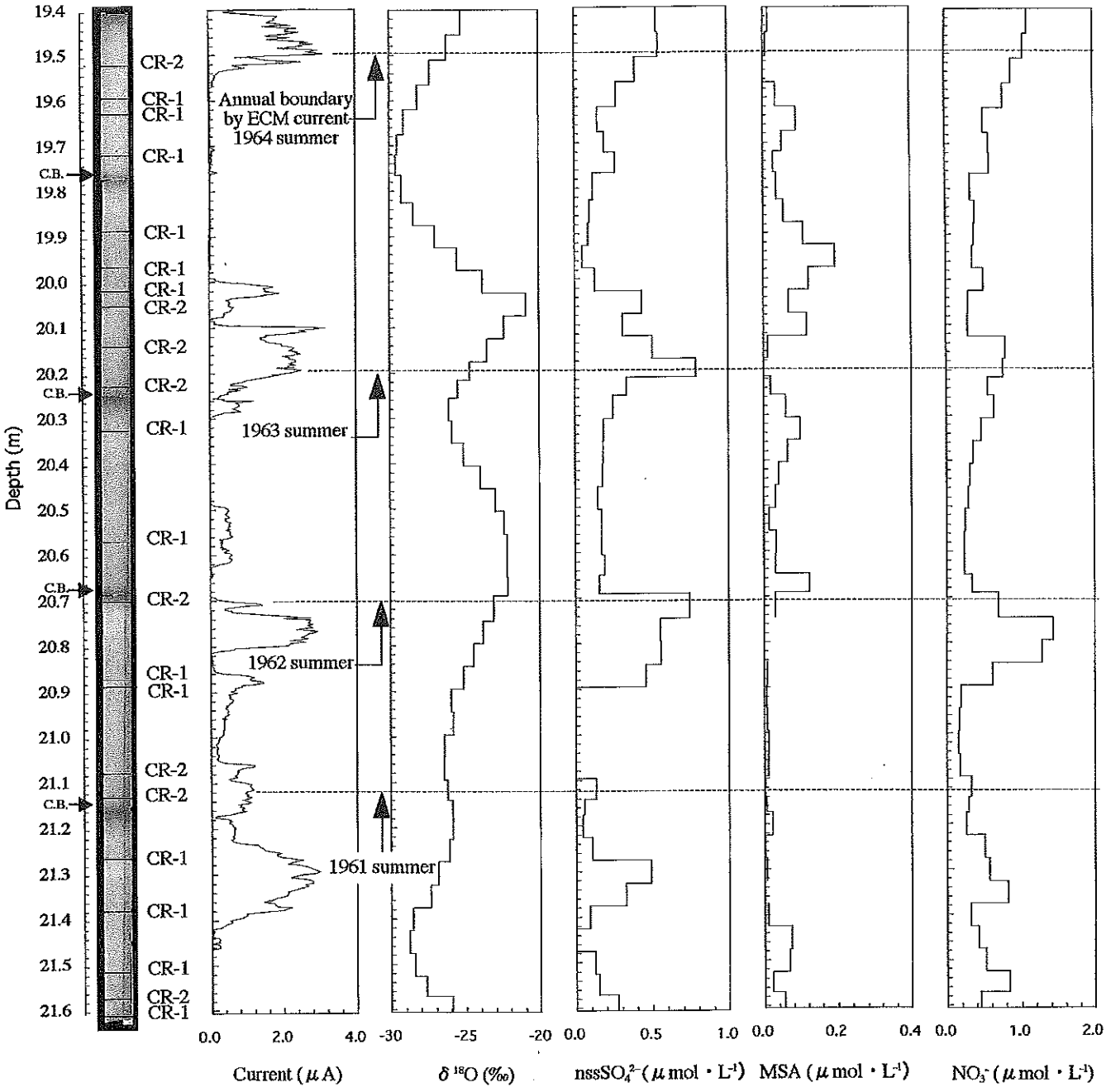

Fig. 4. Profiles of visual stratigraphy, ECM current, $\delta^{18}O$, $nssSO_4^{2-}$, MSA and NO_3^- from 19.40 to 21.60 m. Visual stratigraphy is composed of mosaicked pictures continuously taken by digital video camera along the ice core. Ice crust CR-1 is multi-layered and includes air bubbles. Ice crust CR-2 is identified as probably summer layers at depths of 19.45–19.50, 20.17–20.21 m, 20.74–20.79 and 21.09–21.14 m. C.B. signifies a break in the core.

numbers for each volcanic signal are given in Table 1. Reliability "1" is the highest level, with both the $nssSO_4^{2-}$ and ECM signals in category A. Reliability "2" is the second highest level, corresponding to a single A rating for either the $nssSO_4^{2-}$ or the ECM signal. Reliability "3" is the lowest level, corresponding to remaining events with a B rating for either $nssSO_4^{2-}$ or ECM. Probable source volcanoes for each volcanic signal are investigated using Simkin and Siebert (1994) and Kohno and others (1999) as shown in Table 1.

The symbol "?" is added at the end of the names of the source volcanoes for which the reliability of the signals is "3". It is possible that signal b originates from an eruption by Nevado del Ruiz, Colombia, in 1985 (volcanic explosivity index (VEI) = 3), and signal 1 from Purace, Colombia, in 1869 (VEI = 3). The difference between ages counted by ECM current and volcanic eruption years is also shown in Table 1. The age difference is in the range 0 to +3, which is on the same order as the transportation time from volcanoes to the Antarctic ice sheet.

3.3. Dating by ECM current, visual stratigraphy, tritium content, stable isotopes and major chemical ions

ECM was carried out continuously for the H72 ice core. Nishio and others (2001) describe the instrumentation and the analytical procedure used. We can detect the acidity of an ice core with high resolution by ECM current (Hammer, 1980), and obtain the total amount of H^+ ions (Hammer, 1989). There are seasonal variations of acidity in snowfall. For instance, high sulfuric acid related to regional oceanic production of sulfur-rich gases, methanesulfonic acid (MSA), is generally detected in January around the Antarctic coastal

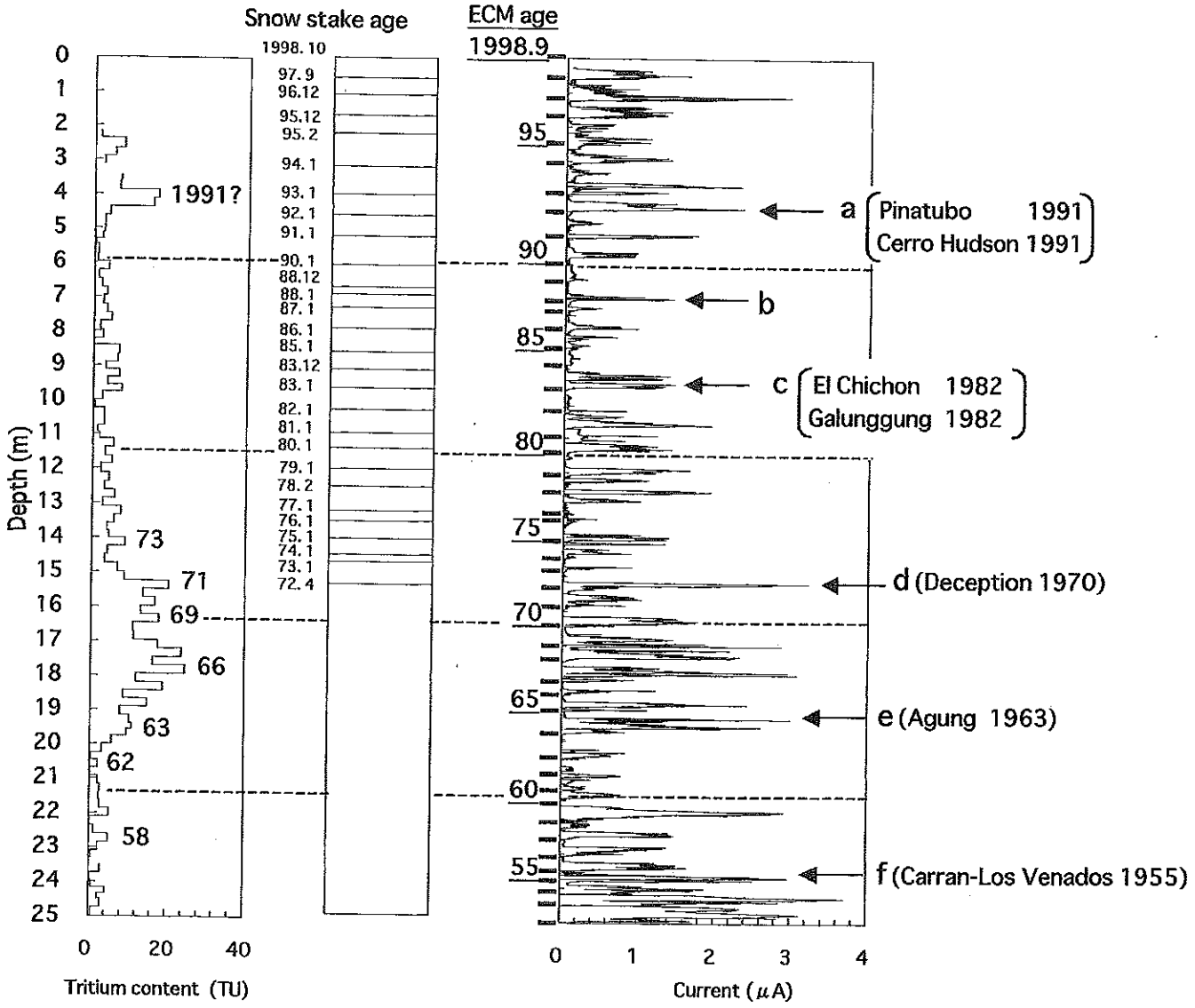

Fig. 5. Comparison of dating with tritium, snow-stake record and ECM from snow surface to 25 m depth. The solid line indicates annual boundary detected by ECM current with visual stratigraphy (CR-2). Arrows show the ages measured by snow stakes. The tritium profile is compared with ECM ages from the surface to 25 m depth. Seven tritium peaks are inferred from the South Pole (Jouzel and others, 1979) except for the unknown peak of 1991.

region (Legrand and others, 1999). These seasonal characteristics are used to detect summer layers in an ice core by ECM.

The characteristics of visual stratigraphy in the H72 ice core are associated with atmospheric conditions. An example is the number of ice-crust layers contained in the H72 ice core. Ice-crust layers are classified into two types according to whether or not the ice crust includes air bubbles, based on observation by eye from digital video images. One is a multi-layered ice crust (CR-1) including air bubbles. The other is a single-layered ice crust (CR-2) without air bubbles, which was probably formed by the melting and refreezing process at the snow surface during the warm period (Narita and Watanabe, 1977). Figure 4 shows profiles of visual stratigraphy, ECM current, $\delta^{18}O$, $nssSO_4^{2-}$, MSA and NO_3^-. Visual stratigraphy is composed of mosaicked pictures, which are continuously taken by digital video camera along the ice core. The high ECM current with ice-crust layer (CR-2) is apparently identified as a summer layer as shown at depths of 19.45–19.50, 20.17–20.21, 20.74–20.79 and 21.09–21.14 m. The $nssSO_4^{2-}$ and NO_3^- concentrations also indicate high peaks as summer layers at the same depths of ice core; on the other hand, the high $\delta^{18}O$ peak is found at slightly shallower depths, so it seems to appear a few months later than the ECM peak. Thus, we count seasonal variations by the high ECM current with ice-crust layer (CR-2) for the whole H72 core, and we define this dating as the ECM age. Although the $\delta^{18}O$ peak indicates seasonal variations in Figure 4, the seasonal variation of $\delta^{18}O$ becomes unclear below about 40 m depth. When the ECM age and the $\delta^{18}O$ age are compared with the time marker of volcanic events listed in Table 1, the dating by the $\delta^{18}O$ age is younger than the ECM age. The comparison for ECM age with the time marker of volcanic events is discussed in section 3.4.

Figure 5 shows tritium content, snow-stake record at H72 (as shown in Fig. 2) and ECM current from surface to 25 m depth. Solid lines below the ECM age indicate the annual-layer boundary detected by ECM current with CR-2 type ice-crust layer. The ECM age agrees with the snow-stake record back to AD 1972 from the surface to 15 m depth. As shown on the left side in Figure 5, we analyzed tritium content from 2.17 to 24.85 m and detected seven tritium peaks at depths of 14.00–14.25, 15.24–15.49, 16.22–16.46, 17.69–17.94, 19.39–19.57, 20.47–20.68 and 22.60–22.85 m. According to AD 1978 pit results at the South Pole (Jouzel

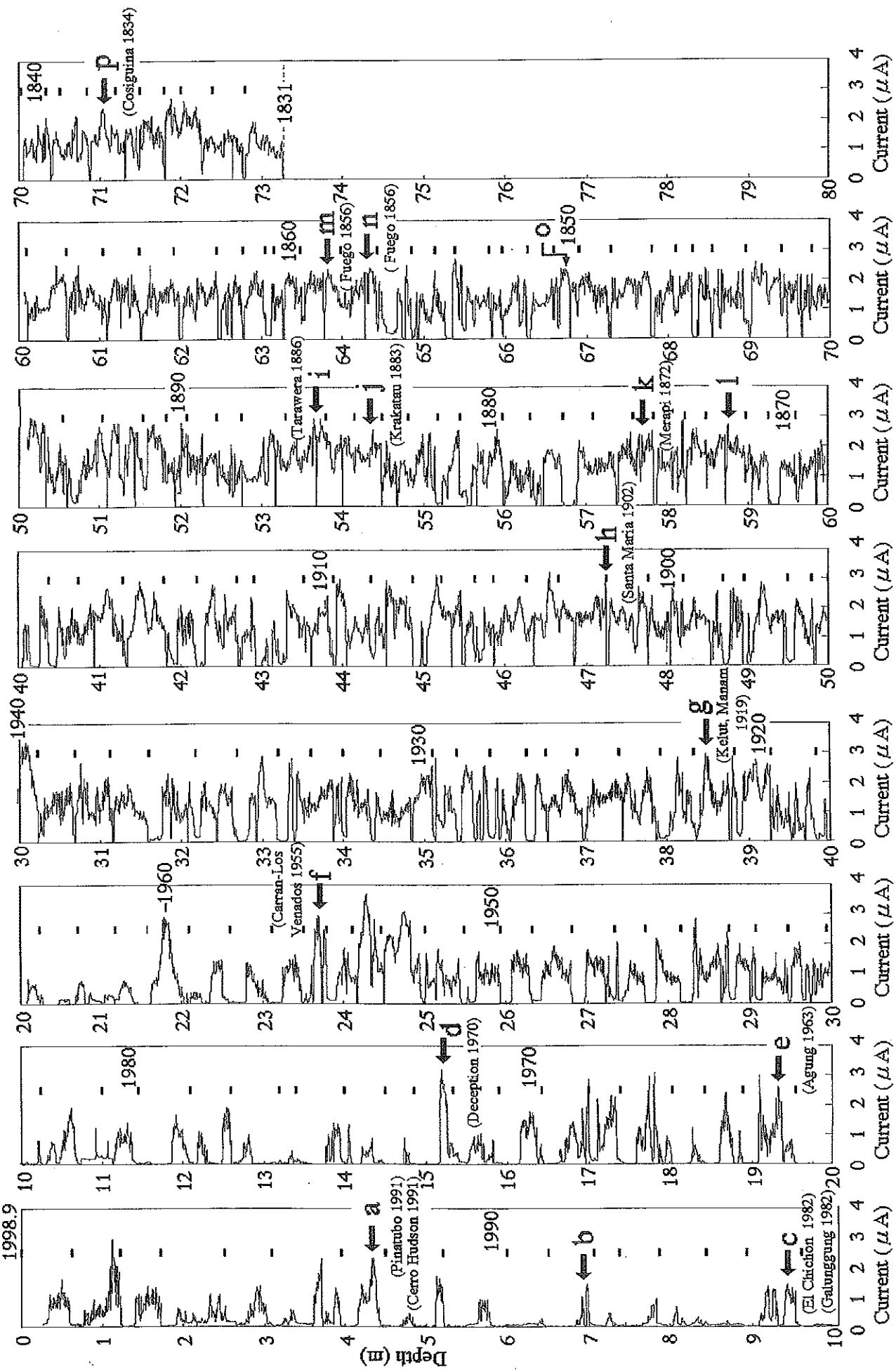

Fig. 6. Profiles of ECM current of the entire H72 ice core. The solid line indicates the annual boundary detected by ECM current with visual stratigraphy. The ECM age was dated as AD 1831 at 73.16 m depth.

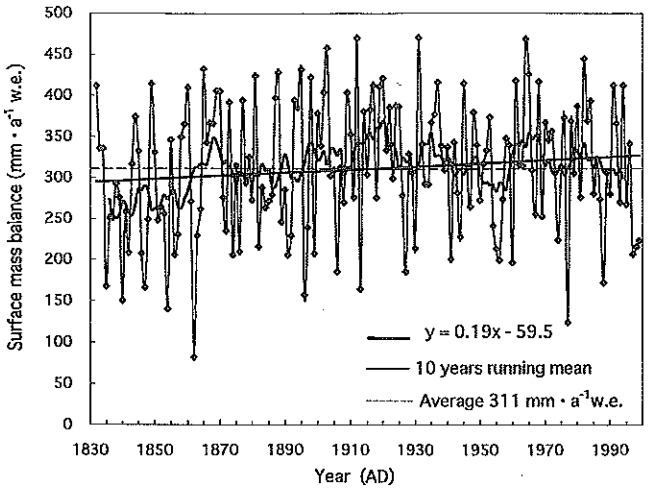

Fig. 7. Surface mass balance in water equivalent at H72, AD 1831–1998. Average surface mass balance is 311 mm a^{-1} w.e. Although the surface mass balance is scattered during the 167 years, the average surface mass balance is almost constant within the 95 % confidence limit.

and others, 1979), we can identify these peaks as AD 1973, 1971, 1969, 1966, 1963, 1962 and 1958, respectively. ECM ages are closely coincident with tritium ages of AD 1963, 1962 and 1958, however; the other four tritium ages of AD 1966, 1969, 1971 and 1973 are about 1 year older than the ECM ages. The reason for the age difference is not clear, since substances from the Northern Hemisphere (NH) will transfer to the interior of the Antarctic ice sheet through the stratosphere, and transportation time from NH to the South Pole is considered to be shorter than that from NH to the coastal region at the H72 site (Kamiyama and others, 1989).

3.4. Annual-layer boundary by ECM current profile

As described in section 3.3, ECM current detects the acidity variations of ice due to seasonal signals such as oceanic sea-salt ions, marine biogenic origin material and background nitric acid, and non-seasonal signals caused by volcanic eruptions. Therefore, we must distinguish between seasonal and volcanic components in the ECM-current data.

To discriminate between the non-seasonal signal and the ECM current, the ECM current is compared with visual stratigraphy in Figure 4. Generally, a winter layer has a low ECM current and includes an ice-crust layer (CR-1) in the visual stratigraphy; on the other hand, high ECM currents often appear not merely in summer layers but also in spring or autumn layers due to oceanic acidity, so that high ECM current is sometimes detected twice or more in an annual layer. An annual boundary, determined by ECM current with visual stratigraphy, is identified at the trans-

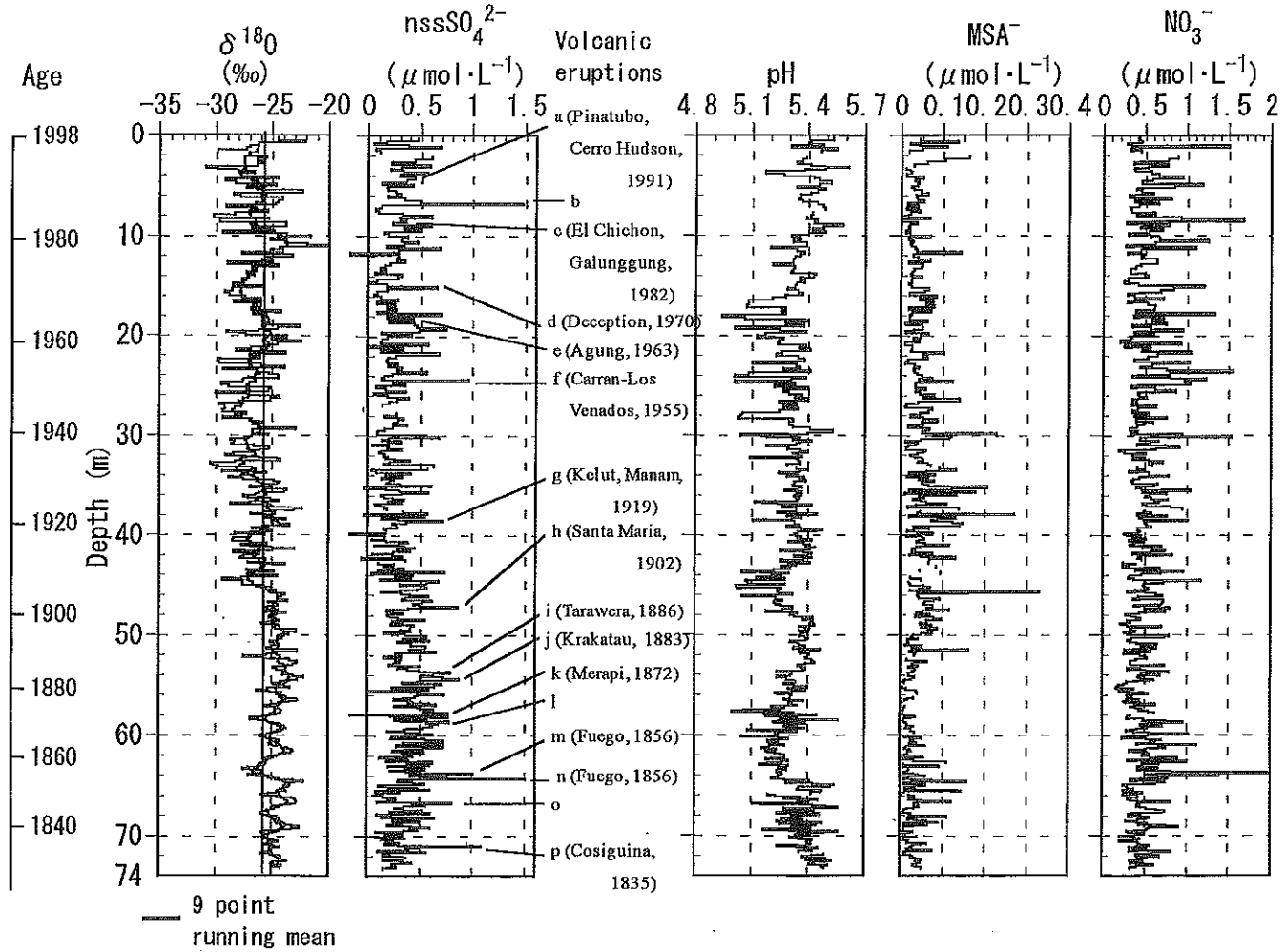

Fig. 8. Profiles of $\delta^{18}O$, chemical constituents ($nssSO_4^{2-}$, MSA and NO_3^-) and pH. Age is due to ECM age. Thick lines in the $\delta^{18}O$ profile show nine-point running means. Possible volcanic eruptions that could give high $nssSO_4^{2-}$ peaks (>0.76 μmol L^{-1}) are given to the right of the $nssSO_4^{2-}$ profile.

ition boundary between low ECM current and high current as indicated in Figure 4.

Figure 6 shows the dating of the entire H72 ice core obtained by ECM currents. The H72 core is dated as AD 1831 by the ECM age at 73.16 m depth. The ECM age agrees with the snow-stake record back to AD 1972 (from the surface to 15 m depth). Furthermore, we compared the ECM age with some time-marker volcanic events to evaluate the ECM age error below 23 m depth. As described in section 3.2, 16 volcanic signals are inferred by ECM current and chemical composition. The ECM age error was estimated by comparing with nine time-marker volcanic events labeled "e, f, g, i, j, l, m, n, p", of which the reliability is 1 or 2 and the probable source volcanoes of which are listed in Table 1. We found that the ECM age indicates the time difference by 0–3 years with the volcanic eruptions in the probable volcanic signals. The acid fallout travel time from the NH to the Antarctic is 2–3 years (Jouzel and others, 1979), and 0–2 years from the Equator to the Antarctic, so the maximum ECM age error is probably 1–3 years at 73.285 m depth.

4. RESULTS AND DISCUSSION

4.1. Time series of surface mass balance

Using the annual-layer boundaries described in section 3, we can determine the surface mass-balance variation over the past 167 years. Figure 7 shows the time series of annual and 10 year averaged surface mass balance. The time series of the yearly surface mass balance at H72 shows a slight increase, with 19 mm (100 years)$^{-1}$ w.e. over the last 167 years, but on the basis of t-distribution analysis this trend is not significant. Average surface mass balance is 311 mm a^{-1} w.e. for AD 1831–1998, which is in good agreement with the annual accumulation of 317 mm a^{-1} w.e. obtained by the empirical densification method described in section 3.1, and the value of 307 mm a^{-1} w.e. obtained by snow-stake data for AD 1973–98.

4.2. Characteristics of isotopes and chemical condition for the last 167 years

Figure 8 shows the oxygen isotope ratio ($\delta^{18}O$), nssSO_4^{2-}, pH, MSA and NO_3^-. These values were continuously measured from surface to bottom at an average interval of 16.3 cm; a total of 450 samples were measured. Analytical methods are described in detail in Nishio and others (2001). In Figure 8, the ages are ECM ages described in section 3; the thin line in the $\delta^{18}O$ profile shows raw data, and the thick line indicates the nine-point running mean of raw data. The vertical solid line indicates the average value as −25.5‰. For the oxygen isotope record, a significant trend to lower values, with a negative gradient of 1.7‰ (100 years)$^{-1}$, can be seen in the H72 ice-core record. More detailed oxygen isotope records show a gradual increase from AD 1840 to 1880, and afterward a gradual decrease to about AD 1900; subsequently, during the 20th century, the isotope record seems to oscillate at an interval of about 20 years. According to previous studies, $\delta^{18}O$ in an ice core is related to the temperature (Johnsen and others, 1989), sea-ice extent (Kato, 1978; Bromwich and Weaver, 1983) and the seasonal variation of snow accumulation (Steig and others, 1994).

The concentration of nssSO_4^{2-} shows similar variations to $\delta^{18}O$ for AD 1840–1900 and gradually increases from AD 1900 to the present. Some spike-like peaks higher than 2σ (>0.76 μmol L^{-1}) are identified as volcanic eruptions, and the probable source volcanoes are shown in Figure 8. MSA is an atmospheric oxidation product of dimethylsulfide (DMS), which is produced by biological sources in the ocean (Savoie and others, 1992). Fluctuation of MSA is small for all depths, except for some spikes. It appears that the chemical constituents of snow are influenced by the ocean when these anomalous peaks are observed. In previous studies (Fisher and others, 1998), NO_3^- has been found to derive from the oxidation of NO and related species that are produced by anthropogenic combustion sources and natural sources, principally soil emissions, lightning and stratospheric processes (Savoie and others, 1992). In the Arctic region, NO_3^- concentration increases from about AD 1900 with increased consumption of fossil fuel. Although a number of spike peaks of NO_3^- are observed in the H72 core, the basic concentration of NO_3^- is almost constant. The pH value has increased over the last 30 years. Therefore, we consider that the NO_3^- in the spike-like peaks originates from natural sources, and not from anthropogenic combustion sources.

ACKNOWLEDGEMENTS

The authors are indebted to the ice-coring team of JARE-39 for their efforts to obtain the ice core at H72. The following persons are acknowledged for their work in the cold room for H72 ice-core analyses at the National Institute of Polar Research: Y. Iizuka, N. Ishihara, J. Okuyama, M. Shirohada, M. Tagami, K. Watanabe and Li Yuansheng. This research was supported by a Grant-in-Aid for Scientific Research from the Ministry of Education, Science, Sports and Culture, Japan (principal investigator: H. Motoyama, 12680537).

REFERENCES

Ageta, Y., T. Kikuchi, K. Kamiyama and F. Okuhira. 1987. Net accumulation of snow along traverse routes. *JARE Data Rep.* 125, 45–61. (Glaciology 14.)

Ayers, G. P., J. P. Ivey and R. W. Gillet. 1991. Coherence between seasonal cycles of dimethyl sulphide, methanesulphonate and sulphate in marine air. *Nature*, 349(6308), 404–406.

Azuma, N. *and 6 others.* 1997. Net accumulation of snow by the stake method. *JARE Data Rep.* 223, 5–39.

Bromwich, D. H. and C. J. Weaver. 1983. Latitudinal displacement from main moisture source controls $\delta^{18}O$ of snow in coastal Antarctica. *Nature*, 301(5896), 145–147.

Clausen, H. B. *and 6 others.* 1997. A comparison of the volcanic records over the past 4000 years from the Greenland Ice Core Project and Dye 3 Greenland ice cores. *J. Geophys. Res.*, 102(C12), 26,707–26,723.

Fischer, H., D. Wagenbach and J. Kipfstuhl. 1998. Sulfate and nitrate firn concentrations on the Greenland ice sheet. 2. Temporal anthropogenic deposition changes. *J. Geophys. Res.*, 103(D17), 21,935–21,942.

Fujii, Y. 1978. Net accumulation of snow by stake method in 1977. *JARE Data Rep.* 48, 3–50. (Glaciology 6.)

Fujii, Y., K. Kawada, M. Yoshida and S. Matsumoto. 1986. Net accumulation of snow along traverse routes in Mizuho Plateau. *JARE Data Rep.* 116, 46–61. (Glaciology 13.)

Fujii, Y., H. Motoyama and N. Azuma. 1995. Net accumulation of snow on Mizuho Plateau. *JARE Data Rep.*, 201, 7–26. (Glaciology 22.)

Hammer, C. U. 1980. Acidity of polar ice cores in relation to absolute dating, past volcanism, and radio-echoes. *J. Glaciol.*, 25(93), 359–372.

Hammer, C. U. 1989. Dating by physical and chemical seasonal variations and reference horizons. *In* Oeschger, H. and C. C. Langway, Jr, *eds. The environmental record in glaciers and ice sheets.* Chichester, etc., John Wiley and Sons, 99–121.

Herron, M. M. and C. C. Langway, Jr. 1980. Firn densification: an empirical model. *J. Glaciol.*, 25(93), 373–385.

Japanese Antarctic Research Expedition. 1999. *Activity report on the 39th Japanese Antarctic Research Expedition.* Tokyo, National Institute of Polar Research.

Johnsen, S. J., W. Dansgaard and J. W. C. White. 1989. The origin of Arctic precipitation under present and glacial conditions. *Tellus*, 41B(4), 452–468.

Jouzel, J., L. Merlivat, M. Pourchet and C. Lorius. 1979. A continuous record of artificial tritium fallout at the South Pole (1954–1978). *Earth Planet. Sci. Lett.*, **45**(1), 188–200.

Kamiyama, K., Y. Ageta and Y. Fujii. 1989. Atmospheric and depositional environments traced from unique chemical compositions of snow over an inland high plateau, Antarctica. *J. Geophys. Res.*, **94**(D15), 18,515–18,519.

Kamiyama, K., T. Furukawa, H. Maeno, T. Kishi and M. Kanao. 1994. Net accumulation of snow by stake method. *JARE Data Rep.* 194, 30–51. (Glaciology 21.)

Kato, K. 1978. Factors controlling oxygen isotopic composition of fallen snow in Antarctica. *Nature*, **272**(5648), 46–48.

Kobayashi, S., T. Ohata, N. Ishikawa, K. Matsubara and S. Kawaguchi. 1982. Net accumulation along the routes S, H, Z, G and Y. *JARE Data Rep.* 63, 3–15. (Glaciology 8.)

Koga, S. and H. Tanaka. 1996. Simulation of seasonal variations of sulfur compounds in the remote marine atmosphere. *J. Atmos. Chem.*, **23**, 163–192.

Kohno, M., Y. Fujii, M. Kusakabe and T. Fukuoka. 1999. The last 300-year volcanic signals recorded in an ice core from site H15, Antarctica. *Seppyo*, **61**(1), 13–24.

Legrand, M. R. and R. J. Delmas. 1987. A 220-year continuous record of volcanic H_2SO_4 in the Antarctic ice sheet. *Nature*, **327**(6124), 671–676.

Legrand, M., E. Wolff and D. Wagenbach. 1999. Antarctic aerosol and snowfall chemistry: implications for deep Antarctic ice-core chemistry. *Ann. Glaciol.*, **29**, 66–72.

Moore, J. C., H. Narita and N. Maeno. 1991. A continuous 770-year record of volcanic activity from East Antarctica. *J. Geophys. Res.*, **96**(D9), 17,353–17,359.

Motoyama, H., H. Enomoto, M. Miyahara and J. Koike. 1995. Net accumulation of snow by stake method. *JARE Data Rep.* 202, 4–25. (Glaciology 23.)

Motoyama, H., Y. Kawamura, M. Kanao, N. Hirasawa, S. Kaneto and T. Yamanouchi. 1999. Net accumulation of snow. *JARE Data Rep.* 239, 6–36. (Glaciology 28.)

Nakawo, M., H. Narita and T. Isobe. 1984. Net accumulation of snow along traverse routes in Mizuho Plateau. *JARE Data Rep.* 96, 55–65. (Glaciology 11.)

Narita, H. and O. Watanabe. 1977. Photographs of vertical section of firn. *JARE Data Rep.* 36, 126–138. (Glaciology 4.)

Nishio, F. 1978. Net accumulation of stake measurements in 1975–1977. *JARE Data Rep.* 44, 2–40. (Glaciology 5.)

Nishio, F. and H. Omae. 1989. Net accumulation of snow along traverse routes between Syowa station and Mizuho station in 1987–88. *JARE Data Rep.* 148, 42–50. (Glaciology 17.)

Nishio, F., H. Omae and K. Osada. 1988. Net accumulation of snow along traverse routes. *JARE Data Rep.* 137, 35–46. (Glaciology 16.)

Nishio, F. *and 7 others*. 2001. [Basic analytical procedure for Antarctic shallow ice cores: methodology and instrumentation.] *Seppyo*, **63**(1), 49–63. [In Japanese with English summary.]

Osada, K. 1994. Seasonal variations of major ionic concentration levels in drifting-snow samples obtained from east Dronning Maud Land, East Antarctica. *Ann. Glaciol.*, **20**, 226–230.

Satow, K. 1977. Net accumulation of snow measured (in 1974–1975) by stake method. *JARE Data Rep.* 36, 36–58. (Glaciology 4.)

Satow, K. 1978. Distribution of 10 m temperatures in Mizuho Plateau. *Natl. Inst. Polar Res. Mem.*, Special Issue 7, 63–71.

Satow, K., H. Nishimura and J. Inoue. 1983. Net accumulation along traverse route routes. *JARE Data Rep.* 82, 4–49. (Glaciology 9.)

Savoie, D. L., J. M. Prospero, R. J. Larsen and E. S. Saltzman. 1992. Nitrogen and sulfur species in aerosols at Mawson, Antarctica, and their relationship to natural radionuclides. *J. Atmos. Chem.*, **14**(1–4), 181–204.

Shiraiwa, T. *and 8 others*. 1996. Net accumulation of snow by the stake method. *JARE Data Rep.* 211, 5–30. (Glaciology 25.)

Simkin, T. and L. Siebert. 1994. *Volcanoes of the world. Second edition.* Tucson, AZ, Geoscience Press.

Steig, E. J., P. M. Grootes and M. Stuiver. 1994. Seasonal precipitation timing and ice core records. *Science*, **266**(5192), 1885–1886.

Takahashi, S. 1984. Net accumulation of snow by stake method in 1982. *JARE Data Rep.* 94, 15–61. (Glaciology 10.)

Wada, M., T. Yamanouchi and S. Mae. 1981. Net accumulation along the routes S, H, Z, G and Y. *JARE Data Rep.* 63, 2–11. (Glaciology 7.)

Watanabe, O. 1978. Distribution of surface features of snow cover in Mizuho Plateau. *Natl. Inst. Polar Res. Mem.*, Special Issue 7, 154–181.

Watanabe, O., T. Furukawa and S. Fujita. 1990. Net accumulation of snow along traverse routes in Mizuho Plateau. *JARE Data Rep.*, **156**, 33–51. (Glaciology 18.).

Yamada, T., H. Narita, F. Okuhira, H. Fukutani, I. Fujisawa and T. Shiratsuchi. 1975. Net accumulation of snow by stake measurements in Soya coast–Mizuho Plateau in 1971–1972. *JARE Data Rep.*, **27**, 10–67. (Glaciology).

Yokoyama, K. 1975. Net accumulation of snow by stake measurements. *JARE Data Rep.*, **28**, 62–82. (Glaciology).